Vol. 601: 185–201, 2018
https://doi.org/10.3354/meps12651

MARINE ECOLOGY PROGRESS SERIES
Mar Ecol Prog Ser

Published August 9

# Oceanographic, acoustic, and remote approaches reveal the spatio-temporal dynamics of blackfin snapper at an aggregation site in Palau

**Megan Cimino[1,*], Patrick Colin[2], Travis Schramek[1], Steven Lindfield[2], Michael Domeier[3], Eric Terrill[1]**

[1]Scripps Institution of Oceanography, University of California at San Diego, La Jolla, CA 92093, USA
[2]Coral Reef Research Foundation, Koror, PW 96940, Palau
[3]Marine Conservation Science Institute, Fallbrook, CA 92028, USA

ABSTRACT: Forming spawning aggregations is a critical life-history activity for fish, but it is unclear what physical conditions are associated with fish behavior at specific sites. The habitat, movements and distribution of blackfin snapper *Lutjanus fulvus* at a monthly aggregation site in Palau were studied using a combination of instruments and approaches, including active/passive acoustics, time-lapse cameras, an autonomous underwater vehicle, current profilers, and high resolution bathymetry. We found that *L. fulvus* predictably form a large pre-spawning aggregation of an estimated 15 000 fish in a small zone (10s of m) in a tidally forced channel. The aggregation spans 125 m along the northern channel wall, with the highest densities of fish from 9 to 13 m and <15 m from the wall where current velocities are <0.25 m $s^{-1}$. The aggregation occurs within an indent in the channel wall where an abrupt change in bathymetry creates a visible eddy-like feature during outgoing tides. The aggregation forms year-round, for 6 d each moon cycle, starting 1 d before the full moon to 4 d after. During the study, 4 tagged fish returned to the site for 6 consecutive lunar cycles; however, residency times within aggregation periods was ~1.5 d on average. Densely aggregated fish were present during the day, but migration patterns of tagged fish revealed regular evening migrations to and from the channel mouth, consistently at the highest tide of the day, a behavior assumed for spawning. These observations reveal some physical processes and biological patterns surrounding the formation and function of fish aggregations.

KEY WORDS: Spawning aggregation · Fish · Telemetry · Acoustics · AUV



## INTRODUCTION

Identifying the underlying physical conditions that are associated with animal behavior is necessary for understanding a species' environmental preferences, identifying threats from climate variation and ultimately, protecting a species' habitat. Many fishes form large schools for protection against predation, to migrate with increased hydrodynamic efficiency, and to enhance reproductive or foraging success. Fish spawning aggregations (FSAs), a type of school, are predictable in time and space, result in a mass point source for eggs and larvae, and potentially enhance reproductive success (Domeier & Colin 1997, Domeier 2012). Fisheries often target these large, predictable concentrations of fish in an unsustainable way (Sala et al. 2001, Sadovy & Domeier 2005). It is often unclear what physical conditions are associated with FSA occurrence and what conditions are critical to their continued existence (Domeier 2012). FSAs are biologically significant since individuals halt their normal routine to migrate, often for considerable distances, and to spawn.

*Corresponding author: mcimino@ucsd.edu

Strategies when forming FSAs are diverse with large variation between fishes, sites, and environmental conditions. There are 2 general types of FSAs: transient and resident, although distinctions between them have blurred somewhat with the discovery that some species have elements of both in their reproductive activities (Domeier 2012). Transient aggregations draw individuals from a large area, but generally occur seasonally with a lunar phase component for many coral reef fishes. In comparison, resident aggregations occur regularly (often daily) and involve shorter migration distances (Domeier & Colin 1997, Domeier 2012).

Present knowledge indicates that different species (with and without FSAs) spawn with particular periodicities (monthly, seasonally, yearly). Spawning by aggregating species is often associated with a particular physical feature, a certain time of day or on a specific lunar or tidal cycle (Nemeth 2005, Heyman & Kjerfve 2008). However, for many families and species, understanding the role of spawning aggregations in reproductive success is still in the 'discovery phase', with a need to fill large gaps in this information to put the phenomenon in ecological perspective and to understand the diversity in this life-history activity, the geographic scope of the lifecycle, and the evolution and importance of reproductive variability.

Snappers (family Lutjanidae) are found worldwide in warm seas (Allen & Talbot 1985), and the few species in the western Pacific with documented spawning behavior are known to form FSAs, such as the twin spot snapper *Lutjanus bohar* and threadfin bream *Symphorichthys spilurus* (Sakaue et al. 2012, 2016). In Palau, a spawning aggregation (spawning not directly observed) of the blackfin snapper *Lutjanus fulvus* was documented based on the presence of large numbers of fish in a reef channel and females with hydrated eggs in the afternoon (an indicator of imminent spawning) (Domeier 2012, Sadovy de Mitcheson & Colin 2012). Visual observations through 2 yr of continuous monthly visits and other periodic checks since 2007 revealed the year-round presence of the aggregation for a few days just after the full moon (Sadovy de Mitcheson & Colin 2012, P. Colin unpubl. data). *L. fulvus* are small (max. size 34 cm; Allen & Talbot 1985) and of minor fishing importance throughout their range (e.g. Sadovy 2007), with nothing else known regarding their spawning biology.

This aggregation of *L. fulvus* in the channel is intriguing for 3 reasons. First, there are no records of traditional knowledge regarding this aggregation (Johannes 1981, Sadovy 2007). Second, although the actual spawning location is unknown, the fish aggregate nearly 1.5 km from the open ocean on only one side of the channel (Sadovy de Mitcheson & Colin 2012, see Fig. 1). Aggregating that far inside the channel mouth does not seem advantageous because fish would have to travel a further distance to arrive at the channel mouth, which is a common fish spawning location that can enhance egg dispersal on falling tides. Third, the location of the *L. fulvus* aggregation lacks distinct features (e.g. promontory, ridge, large pinnacle) attractive to aggregating fish. Thus, this aggregation area contradicts some common characteristics of such sites, drawing into question the environmental cues related to its use as an aggregation site. In this study, we used a combination of instruments and approaches, including active and passive acoustics, time-lapse cameras, an autonomous underwater vehicle (AUV), current profilers, and high-resolution bathymetry to understand *L. fulvus* aggregation habitat characteristics and selection, as well as fish movements and distribution within the vicinity of the channel (see Table S1 in Supplement 2 at www.int-res.com/articles/suppl/m601p185_supp.pdf). There is currently no fishing pressure on this aggregation, so studying its characteristics on multiple scales can lead to a greater general understanding of undisturbed FSA behaviors and help to inform management of *L. fulvus* habitat use patterns in the future.

## MATERIALS AND METHODS

### Study site

The movements, distribution, and abundance of *Lutjanus fulvus* were studied at an aggregation site in West Channel ('Toachel lengui' in Palauan), in the western barrier reef of the main Palau island group (Fig. 1). The channel is about 4 km long and 400 m wide, bisecting the barrier reef from the ocean slope to the inner lagoon area. The barrier reef flat along its edges is shallow (~1 m deep at low tide), but the sides of the channel slope at roughly 30 to 45° to a depth of 70 to 90 m in the channel center. Aerial photographs and satellite images were used to map and document the study area (Fig. 1). The channel sides and adjacent barrier reef flats have well developed reef structures, while the deep channel bottom is largely devoid of such features.

Bathymetry of West Channel and the surrounding region was mapped by merging multiple datasets, including airborne Light Detection and Ranging

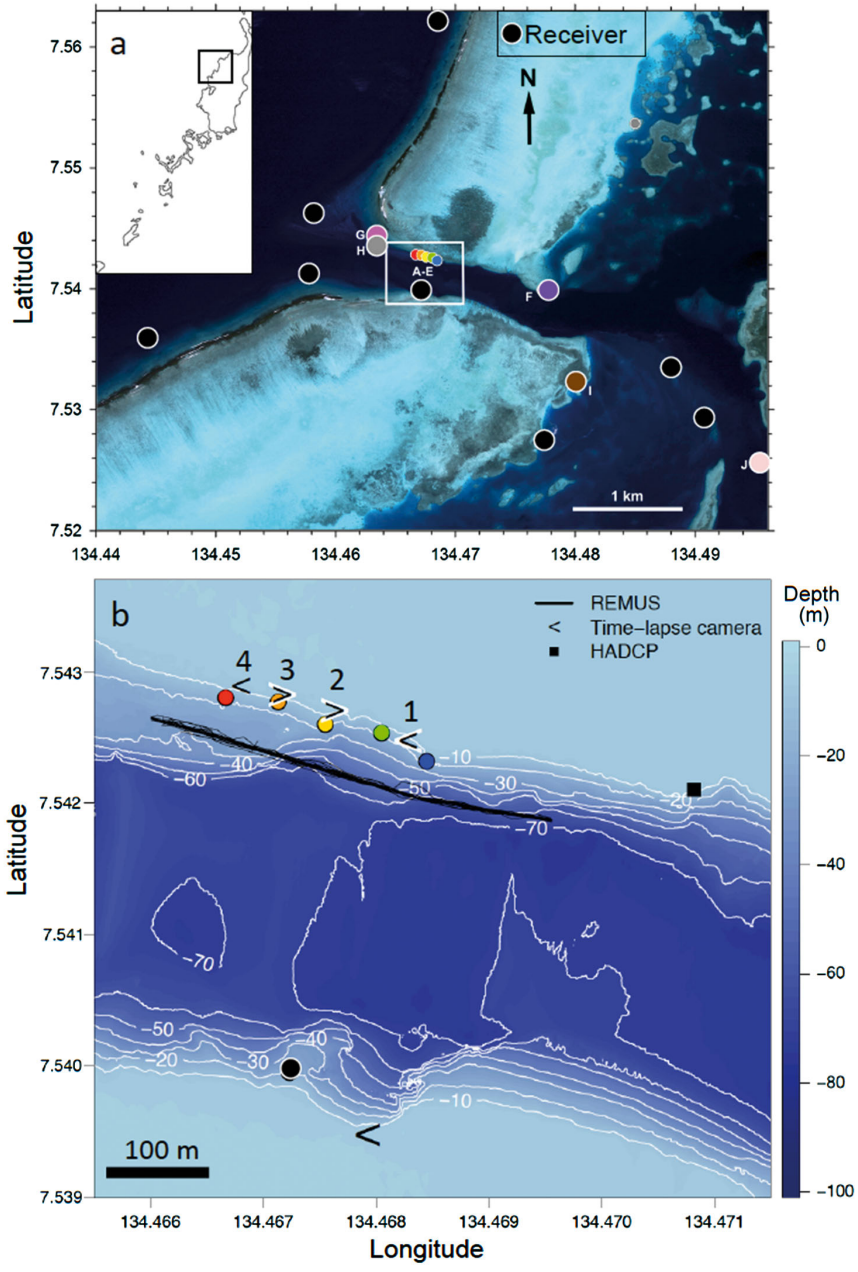


Fig. 1. (a) Quick bird satellite imagery of West Channel, located in the northwest Republic of Palau, with the location of underwater VEMCO acoustic receivers. Colored circles with letters A–J are receivers that detected *Lutjanus fulvus* (see Figs. 2 & S4 in Supplement 3 at www.int-res.com/articles/suppl/m601p185_supp.pdf), while black circles are receivers that did not. Within the white box is the blackfin snapper aggregation site. (b) Close-up of the aggregation site in (a), showing the same receiver locations, the location of REMUS AUV missions, GoPro time-lapse camera locations (direction of arrow indicates the direction the camera was facing), and a horizontal acoustic Doppler current profiler (HADCP) deployed in 2011 and 2012. White arrows indicate time-lapse camera deployments in 2011 while black represents 2012. The southernmost time-lapse camera was mounted on a pole above the sea surface

(LIDAR) flown in 2004 by the Naval Oceanographic Office, boat-based single point sonar (Colin 2009), and multi-beam/Echoscope sonar from 2012. The resultant mapping allowed for examination of the effects of bottom and channel wall topography on current patterns and their influence on the location of the aggregation. Data outside of the channel was from ETOPO1, a 1 arc-minute global relief model (https://www.ngdc.noaa.gov/mgg/global/global.html).

## Data collection and analysis

An overview of our approaches to detect the presence and movements of fish and document their habitat is included in Table S1 as well as instrument deployment dates and rationale.

### Acoustic tagging

Individuals were acoustically tagged to study their spatial and temporal movements via a network of acoustic receivers established within the vicinity of West Channel (Fig. 1a). A total of 22 fish were captured at the aggregation site by hook and line on the evening of 31 October 2012, transported in a live tank to the Palau Community College aquaculture facility (3 km away) and held overnight in large holding tanks with running seawater. The next morning, after measuring total and standard length, the 20 surviving fish had acoustic tags surgically implanted via a small incision made in the left side of the gut, tag insertion, and closing with a single stitch. Each operation required only 2 min. During tag insertion, the gender of the fish was determined by looking at the gonad. Because the fish were ripe, ovaries and testes were visible and males would exude sperm when the abdomen was gently squeezed. Due to the relatively small size of adults (19 to 26 cm total length, mean 22 cm; see Fig. S1 in Supplement 3), we used small, short-lived acoustic tags (V9-2H, VEMCO; 9 mm diameter, 29 mm long, 2.9 g in seawater). Collections were permitted under a Marine Research Permit from the Palau National Government.

The tags transmitted uniquely coded signals every 50 to 130 s at a frequency of 69 kHz and power level of 151 dB (re 1 µPa at 1 m) with an expected tag life of 147 d. We describe the expected detection range below. At mid-day after surgery, the fish were transported in a live tank back to the same site and released in groups. A diver observed that all fish immediately swam to the bottom, appeared to behave normally, and within a few minutes merged into the general aggregation. No predation attempts were observed.

An array of 19 passive acoustic receivers (VR2, battery life of ~18 mo; VEMCO) deployed in April 2012 was recovered in October 2013. All were deployed within about 10 km of the aggregation site at depths of 9 to 12 m and 24 m for receiver H (Fig. 1a). An omnidirectional hydrophone recorded fish transmitter codes when within the detection range of the receivers. The array had 5 receivers at the aggregation site, approximately 50 m apart along the side of the channel (Fig. 1b) to determine presence/absence at the site. Other receivers were located within about 10 km of the aggregation site to examine dispersal and migration of the tagged fish. The receivers (pointing upward) were placed at the end of vertical poles inserted into reef crevices and secured to the reef structure with tie wraps. They were 2 m above the surrounding structure and were well exposed from all directions. It should be noted that there were large gaps in our receiver array, which limited our ability to track fish movements between receivers located outside of the aggregation site.

We investigated the transmitter detection range in our system using a test tag pinging at 1 Hz that was left at receiver D for ~10 min. This short test was not sufficient for statistical analyses or to provide a conclusive detection range, but the few observations revealed that the detection range was at least 106 m at times (distance from receiver D to B, the furthest detection) but likely less than 158 m (distance from receiver D to A, where it was not detected). In addition, throughout the study, one transmitter within a fish was occasionally detected by 2 receivers at the aggregation site spaced 50 m apart at the same time, but never 3 receivers simultaneously. This suggests the detection range was <100 m during the time that the fish were at the aggregation site and reveals our array had limited ability to detect fish given the large gaps between receivers and the small detection range. Overall, this is a smaller detection range compared to past studies using this tag type (V9-2H) that showed the majority of detections were from a distance <300 m (How & de Lestang 2012, Bacheler et al. 2015, Özgül et al. 2015) but similar to Kawabata et al. (2011) showing a range of ~100 m.

We investigated the location of acoustic detections in multiple ways. First, we determined the proportion of detections by receiver (raw data). Second, detections were reduced to modal locations by hour (detection events), if the fish was detected during that time. In the infrequent occurrence of an hourly mode occurring at multiple locations, the hourly modal location was assigned at random to 1 of the 2 locations with the highest number of detections (Breece et al. 2013). For each fish, the percentage of detections occurring on each receiver was calculated by dividing the number of detections on that receiver by the total number of detections for that fish. Visualizing the data in multiple ways allowed for a clear, quantitative determination of areas most frequently utilized.

To understand the distribution of acoustic detections by hour, we calculated the kernel density estimate of detections by grouping detections by the number of days after the full moon. We used a 2-dimensional kernel density estimation with an axis-aligned bivariate normal kernel (Venables & Ripley 2002). We also tested for differences in fish detection hour by the number of days after the full moon. We used a linear mixed model (LMM) to account for repeated measurements on an individual fish and the correlation between these repeated measurements. We treated the individual as a random effect using the 'nlme' package (Pinheiro et al. 2010) in R (R Core Team 2013). Results were considered statistically significant when $p < 0.05$.

### Time-lapse photography

We deployed multiple time-lapse camera systems (GoPro Hero 2 cameras with external battery packs) at the aggregation site with ~50 m spacing between cameras (Fig. 1b) to take photos at 1 min intervals for several days. Systems were deployed prior to arrival of the aggregating fish and remained in place until the aggregation had ceased. Three systems were deployed during 19 to 24 March 2011, and 4 during 5 to 15 March 2012 (see Fig. 4 for deployment time and depth ). Time-lapse photos were manually examined for presence/absence of *L. fulvus*. This system was limited to daylight hours because all nighttime photos were black. Because single photos often had hundreds of fish visible, automated methods for determining fish numbers were unsuccessful (see Fig. S2 in Supplement 3).

An above-water time-lapse camera was attached to a marker pole on the south side of the channel across from the aggregation site (Fig. 1b) on 10 March 2012. It took photos (10 s interval) on the falling tide from 10:20 to 15:10 h (high tide 08:31 h, low tide 14:55 h), documenting an eddy-like feature visible on the sea surface.

### Tide data

Hourly tide level data was obtained from the University of Hawaii Sea Level Center, Global Sea-level Observing System (GLOSS) Core Network (http://uhslc.soest.hawaii.edu/data/?fd). The Palau tide station is located in Malakal Harbor, 22 km from the study site, but previous deployments of pressure loggers at the study site indicated its tidal patterns closely matched Malakal station (Pearson's correlation $R = 0.99$, $p < 0.05$).

### Horizontal acoustic Doppler current profiler

A 307 kHz RD Instruments horizontal acoustic Doppler current profiler (HADCP) was deployed in a flat-bottomed cave located on the side of the near-vertical channel wall at 10.75 m water depth from 5 to 12 March 2012. This was the closest location to the aggregation site that allowed for a secure installation (Fig. 1b). The data were averaged into 1 min ensembles with 20 pings ensemble$^{-1}$ with 1.68 m bins ranging from 3.88 to 141.64 m from the instrument. An internal pressure sensor provided concurrent data on the tides. Current velocities were grouped into tide phase (high, low, outgoing, incoming) based on water level (see Fig. S3 in Supplement 3).

### Thermographs

Onset U-22 HOBO recording thermographs were deployed along the reef wall. Thermographs were deployed at 15, 30, 45, and 57 m from 5 to 12 July 2010 and at 15 m from 8 January to 15 May 2012. Loggers sampled at 12 min intervals in 2012 and at a 30 min interval in 2010.

### REMUS AUV

We used a propeller-driven REMUS-100 AUV to map the distribution and abundance of the *L. fulvus* aggregation on the morning outgoing tides of 21 March 2011, and 8 to 10 March 2012 (full moon period, aggregation present). The REMUS uses a compass for heading, GPS for surface navigation, pressure sensor for depth, Doppler Velocity Log (DVL) for speed and altitude over the seafloor, and acoustic transponders for underwater navigation (Moline et al. 2005). The vehicle ran approximately 400 m long survey lines parallel to the north channel wall ~1.5 km inside the mouth of West Channel (Fig. 1b) at successively deeper depths of 5, 12, and 18 m in 2011, and 5, 9, and 13 m in 2012. The REMUS completed 5 survey lines on 21 March 2011, 6 on 8 March, 5 on 9 March and 3 on 10 March 2012. The missions ranged from 40 min to 2 h (mean 1.5 ± 0.63 h) and travelled at an average speed of 1.1 m s$^{-1}$. The goal was to complete a total of 3 or 6 survey lines d$^{-1}$ once or twice at each depth. The varying number of survey lines on each day was the result of successful vehicle navigation. The strong tidal currents made acoustic navigation challenging and on a few occasions rendered the data unusable. The study area was adequately surveyed (Aglen's ratio = 17; Aglen 1989).

The REMUS measured temperature, salinity, depth (YSI CTD), currents, and acoustic backscatter. An upward- and downward-looking 1200 kHz Teledyne RD Instruments acoustic Doppler current profiler (ADCP) provided estimates of vehicle speed over the bottom and water velocity profiles. The ADCP was configured to sample 60 bins (25 cm bin$^{-1}$) at 1 Hz. ADCP data was grouped into 0.5 m bins and range limits were restricted to 5 m on the upward-looking and 7 m on the downward-looking ADCP due to acoustic noise in the water. All ADCP measurements at depths <3 m were removed due to high surface noise, and measurements from the downward-looking ADCP resulting from bottom reflections were eliminated. We followed the methods of Rogowski et al. (2014) for processing the ADCP data.

A single-beam 217 kHz BioSonics DT-X portable digital scientific echosounder whose transducer was mounted to look horizontally from the port side of the REMUS acoustically mapped fish when the REMUS traveled from west to east along the channel wall. The echosounder has a beam width of 5.7°, a transmit source level of 221.9 dB and receiver sensitivity of −51.5 dB. The transducer had a ping rate of 5 pings s$^{-1}$ and a transmit pulse duration of 0.1 ms. The minimum data collection threshold was −150 dB. Data was obtained within 0 to 104 m from the transducer. Details about acoustic data processing to obtain areal (fish m$^{-2}$) and volumetric (fish m$^{-3}$) estimates of fish

density is included in Section S1 in Supplement 1. As fish density data was not normally distributed, we used a nonparametric Kruskal-Wallis test and a multiple comparison test after Kruskal-Wallis to determine if the distribution of fish density differed between days and depths.

We estimated the abundance of *L. fulvus* with data from acoustics surveys using echo integration outputs. For each day and depth the REMUS sampled, we grouped fish density estimates into 5 m bins as a function of distance along the channel wall from the beginning to the end of the acoustic surveys. We calculated a minimum, mean, and maximum density of fish (fish $m^{-2}$) in each grid cell, as multiple surveys were run at each depth. An evenly spaced vertical grid was created using these 5 m distance bins along the channel wall and 1 m depth bins ranging from 3 to 20 m (visual observations suggest fish inhabit this depth range). We combined all depth observations of fish $m^{-2}$ from each day and spatially interpolated between REMUS survey lines at different depths to obtain a minimum, mean, and maximum estimate of fish abundance for each sampling day. For spatial interpolation, we used kriging, which allows values to be mapped at points without direct observations from neighboring regions using spatial autocovariance (Journel & Huijbregts 1978, Cressie 1988). Ordinary kriging is a well-established method and was performed using the package 'geoR' in R (Ribeiro & Diggle 2001). This method has been used and recommended to determine fish abundance (Bezerra-Neto et al. 2013 and references within). For each survey day, total abundance of minimum, mean, and maximum fish estimates were determined by multiplying density by the area of the grid cell and then summed (Dalen & Nakken 1983). To estimate the total number of *L. fulvus* that visited the aggregation site in an aggregation period, we averaged minimum, mean, and maximum total abundance estimates from all days, respectively, and multiplied by 4 to account for the aggregation lasting 6 d and a fish having an average residence time of 1.5 d determined from acoustic tags (Table 1).

### Dye release experiment

The existence of an eddy-like feature occurring on falling tides, possibly due to the effect of flow hitting abrupt topographic features, was noted. On 19 January 2017, 1 wk after the full moon, we used colored dye (1 kg of UV-degrading uranine dye [TCI America] dissolved in 25 l of seawater) to visualize this flow and determine its relationship to the fish aggregation. Two dye-release experiments were conducted. First, 20 l of dye mixture was released along the north channel wall in a north-to-south line upstream from the eddy-like feature, and second, after this dye was visibly absent from the channel, 5 l of the mixture was released within the northwest corner of the eddy. In Expt 1, the dye was tracked via an aircraft taking photos and an ECO uranine fluorometer (WET Labs), calibrated in the lab prior to the experiment, attached to the side of the boat (<1 m). Only the boat based fluorometer was used in Expt 2. We put 2 current drifters with an attached surface float (hereafter drogues) with a position-logging GPS receiver in the water near the dye release point.

## RESULTS

### Fish movements from acoustic telemetry

Of the 20 fish acoustically tagged in early November 2012, 8 were detected by receivers at the aggre-

Table 1. Arrival and departure hour and day, total days present from first to last detection, and total night hours present (between 19:00 and 06:00 h) at the aggregation site for the 6 telemetered blackfin snappers *Lutjanus fulvus* that were detected at the aggregation site for more than 2 mo from late November 2012 to March 2013

| Snapper tag ID (sex) | Months present at aggregation site | Most frequent arrival day (days after full moon, median arrival hour) | Most frequent departure day (days after full moon, median departure hour) | Unique hours detected at night for the full moon period (mean ± SD) | Days present at aggregation site (mean ± SD) |
|---|---|---|---|---|---|
| 1 (female) | 3 | 1, 02:00 | 2, 14:00 | 0.67 ± 0.58 | 0.76 ± 0.67 |
| 3 (male) | 5 | 1, 07:00 | 3, 16:00 | 1.00 ± 1.22 | 1.88 ± 0.94 |
| 5 (male) | 5 | 1, 06:00 | 3, 10:00 | 1.00 ± 2.24 | 1.89 ± 0.73 |
| 6 (male) | 5 | 2, 07:00 | 3, 15:00 | 0.40 ± 0.89 | 1.42 ± 0.73 |
| 7 (female) | 5 | 2, 02:00 | 3, 16:00 | 5.40 ± 2.41 | 1.58 ± 0.06 |
| 8 (male) | 3 | 2, 06:00 | 3, 18:00 | 2.33 ± 4.04 | 1.41 ± 0.15 |
| Average | | | | 1.80 ± 1.89 | 1.48 ± 0.42 |

gation site during aggregation periods from late November 2012 until March 2013 (Fig. 2a), a period of at least 149 d (1 November to 30 March) and in agreement with the nominal tag life length. These individuals were 22 to 25.5 cm total length, both male and female (see Table S2 in Supplement 2). Notably, 4 fish (tag IDs 3, 5, 6, 7) were detected at the aggregation site in all 6 mo during the full moon period (Fig. 2a), 2 others (fish 1 and 8) were present in 4 mo and a final fish (fish 4) was present in 2 mo. The last tagged fish (fish 2) was detected on receiver E inconsistently for 1.5 mo and appeared to be residing near the aggregation site, but after mid-December 2012, that tag was never detected again (shortly after Typhoon Bopha passed over Palau on 6–7 December). The tag might have been lying on the bottom, likely after a predation event, and was later moved from the area during the storm. No matter the reason, this inconsistent data was removed from further analyses.

The telemetry data was useful for identifying the locations that individuals used in a given full moon period. Fish were detected by 10 of the 19 receivers (Fig. 1a). From late November 2012 to March 2013 (ignoring the data during the tagging period in early November), over 99% of the detections were within

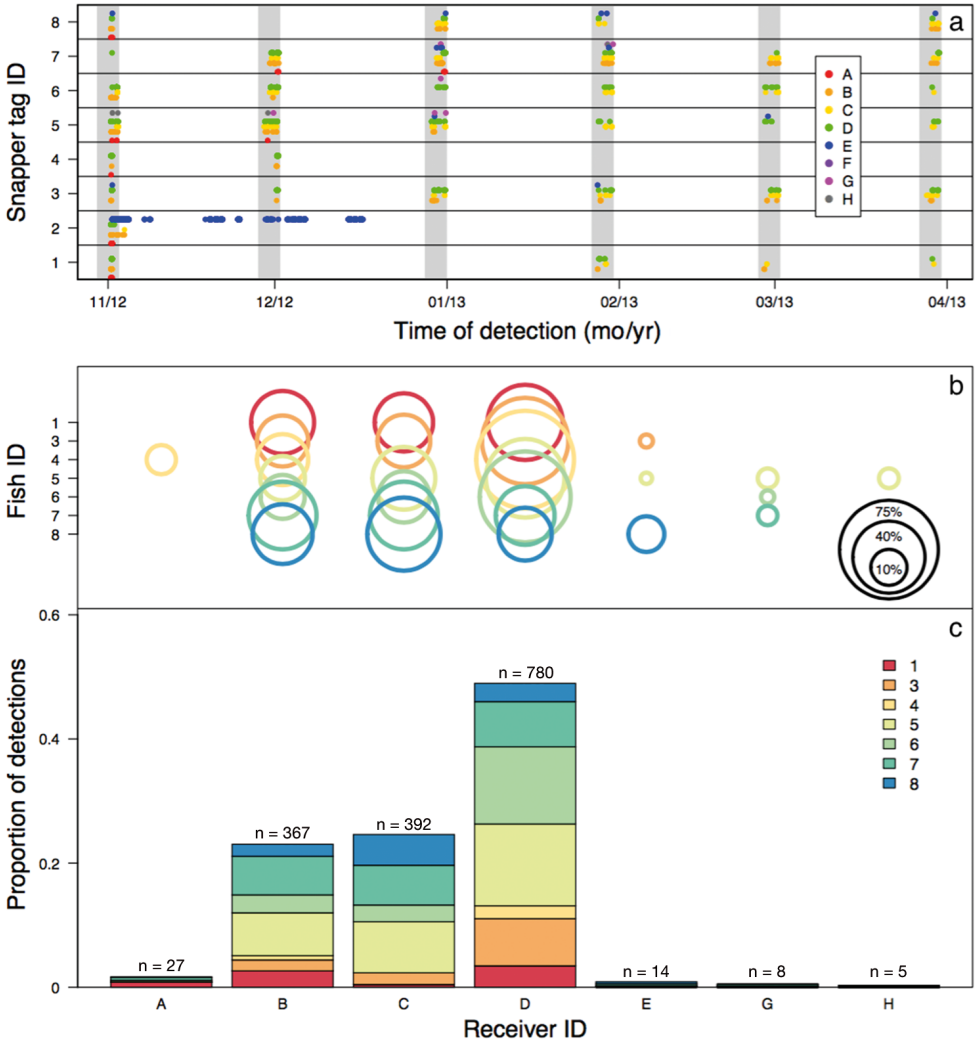


Fig. 2. Presence and absence of telemetered *Lutjanus fulvus* at VEMCO acoustic receivers from November 2012 to March 2013. (a) Time of acoustic detections for each fish at different receivers (A–H). Gray bars indicate the time of the full moon until 4 d after. The color of the receiver matches receiver locations in Fig. 1a. (b) Proportion of hourly snapper detections on each acoustic receiver for each fish. The size of the circle is scaled by the proportion of detections by individual. (c) Proportion of all snapper detections on each acoustic receiver. Fish 2 was not included in (b) or (c). Colors in (b) and (c) correspond to snapper tag ID. Sample size (n) is the number of detections at each receiver. See Fig. S4 in Supplement 3 for detection timing and frequency for snappers that were only detected in early November 2012

Table 2. Local time and date of detections of *Lutjanus fulvus* on receivers G or H and the previous and next detection time and location. The time of the highest tide of the day is included in parentheses under date. A possible interpretation of the fish's behavior is included, given our current knowledge of fish spawning behavior and this aggregation. (–) represents when a fish was not detected again during that full moon period

| Fish tag ID | Date (time of high tide) | Detection time (receiver G or H) | Previous detection time (receiver) | Next detection time (receiver) | Possible interpretation |
|---|---|---|---|---|---|
| 5 | 29 Nov 2012 (19:23) | 18:43 (H) | 18:03 (B) | 30 Nov 06:30 (D) | Spawning movement |
| 5 | 30 Nov 2012 (19:56) | 18:36 (G) | 17:58 (B) | 21:50 (C) | Spawning movement |
| 5 | 29 Dec 2012 (19:42) | 18:46 (G) | 18:11 (E) | 30 Dec 07:01 (D) | Spawning movement |
| 5 | 31 Dec 2012 (20:54) | 19:04 (G) | 17:54 (C) | – | Spawning movement and/or exiting channel |
| 6 | 30 Dec 2012 (20:18) | 21:00 (G) | 16:51 (D) | 31 Dec 08:16 (D) | Spawning movement |
| 7 | 30 Dec 2012 (20:18) | 20:50 (G) | 18:02 (B) | 20:51 (G) | Spawning then loitering near receiver |
| 7 | 30 Dec 2012 (20:18) | 20:51 (G) | 20:50 (G) | 21:01 (E) | Moving back to aggregation site |
| 7 | 29 Jan 2013 (20:43) | 21:04 (G) | 15:30 (B) | 21:12 (H) | Loitering near receiver |
| 7 | 29 Jan 2013 (20:43) | 21:12 (H) | 21:04 (G) | 22:00 (B) | Spawning movement |
| 7 | 30 Jan 2013 (21:21) | 21:20 (G) | 16:59 (C) | – | Spawning movement and/or exiting channel |

the aggregations site (Fig. 2). For hourly modal detections, 5 (fish 1, 3, 4, 5, and 6) of the 8 fish were most frequently detected on receiver D (>50% of the time; Fig. 2b). The remaining 2 fish (fish 7 and 8) had detections more equally spread out between receivers B, C, and D (ranging from 20 to 40%; Fig. 2b). At the site, 49% of all the detections were on receiver D, 25% on C, 23% on B, and 2% on A (Fig. 2c). There were very few detections on receivers G (n = 8) and H (n = 5), which were located close together on the northwest edge of the channel wall, with H being deeper at 24 m (Fig. 1a). Overall, the majority of detections from all fish were located in the middle of the 5 receivers at the aggregation site. Comparatively, the 12 fish that were only detected in early November had more variable behavior, staying at the aggregation site longer than the full moon period or were detected on more distant receivers, but still, 93% of the detections were within the aggregation site (see Fig. S4 in Supplement 3 and Section S2 in Supplement 1 for more details).

Three fish were detected 10 times on receivers G and H (Fig. 2a) near the channel mouth, from late November to January between sunset and midnight (Table 2). We discuss each of the 3 fishes movements separately in Section S3 in Supplement 1. In summary, these fish were detected by receivers G and H near the time of the evening high tide and were always detected back at the aggregation site after high tide, either later that night or at sunrise. These fish were detected at the channel mouth at a similar time from 18:30 to 21:30 h (Table 2). Additionally, fish 5 (male) and fish 7 (female) were both detected at receivers G and H on 2 successive nights within one aggregation period, suggesting fish might make multiple spawning migrations to the channel mouth.

The acoustic telemetry data was useful for examining how long individuals make use of the aggregation site in a given full moon period. The movements of those snappers that displayed consistent site usage (fish 1, 3, 5, 6, 7, and 8; Table 1), appearing at the aggregation site only around the full moon when the aggregation normally occurs, were analyzed and we considered their behavior characteristic of the majority of individuals forming the spawning aggregation. These tagged snappers arrived 1 or 2 d after the full moon and departed 2 to 3 d after the full moon (Table 1). The fish arrived between the hours of 01:00 and 09:00 h (one outlier at 14:00 h), most often between 02:00 and 06:00 h, and on the incoming tide (low tide at ~02:00 h, high tide at ~08:00 h). They departed between 09:00 and 18:00 h, most often between 14:00 and 18:00 h (Table 1), again on the incoming tide (low tide ~15:00 h, high tide ~21:00 h). These fish were only detected at the aggregation site 1, 2, and 3 d after the full moon. The time period from the first to last detection for individuals ranged from 6 h to 2.5 d, averaging 1.48 ± 0.42 d (Table 1). Interestingly, although the receivers spanned a distance of only 207 m, not all fish were detected on all 5 receivers at the aggregation site during a given aggregation period. Individual fish remained near a subset of the receivers (Figs. 2 & S4 in Supplement 3). The first and last detection of each fish during an aggregation period was rarely from the outer receivers (A or E); 96% of the time they were first detected on receivers B to D (B: n = 11; C: n = 5; D: n = 9; E: n = 1), and 85% of the time the last detection was on receiver C or D (B: n = 2; C: n = 10; D: n = 12; E: n = 2).

The majority of the detections at the aggregation site were during the day, beginning around sunrise

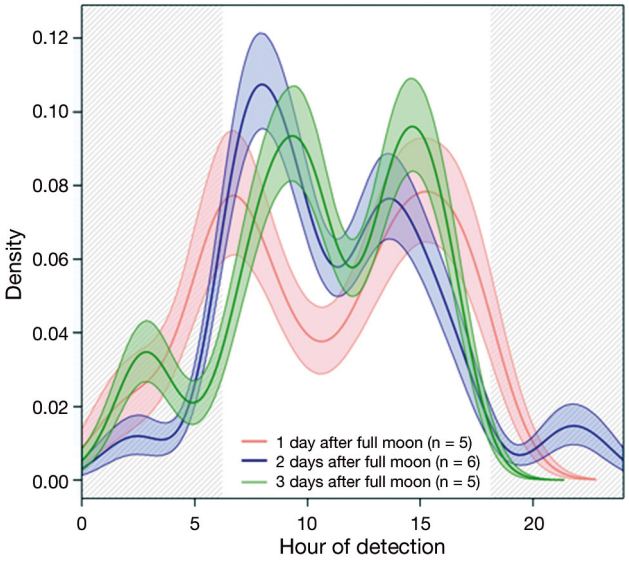


Fig. 3. Kernel density distribution of acoustic detections by hour for *Lutjanus fulvus* detected across more than 2 mo at the aggregation site from late November 2012 to March 2013. Detections are grouped by the number of days after the full moon. The 95% confidence interval is shown around each kernel density estimate. Sample size (n) represents the number of fish detected on that day. The average time between sunrise and sunset is shaded gray (19:00 to 06:00 h). The time of sunrise and sunset varied by only 20 min between December and March

and ending around sunset. When fish were detected at the aggregation site during the night, it was mainly after midnight and on average, for less than 2 h (Table 1). Fish 7 was detected the most times at night (5.40 ± 2.41 h; Table 1). The distribution of detections was not significantly different on different days, whether it was 1, 2, or 3 d after the full moon (LMM $t$-statistic = –0.714, p = 0.48; Fig. 3). There was a bimodal distribution of detections peaking between 07:00 to 09:00 h and 14:00 to 16:00 h (Fig. 3). In general, fish that were only present after the initial tagging in early November also left the aggregation site between sunset and sunrise (Fig. S4 in Supplement 3). This largely agrees with visual observations from the time-lapse cameras.

### Aggregation presence from time-lapse photos

During March 2011 and 2012, the presence or absence of *L. fulvus* aggregations was determined using a series of time-lapse cameras deployed during the full moon in the aggregation area (Fig. 1b). Visibility in the channel was tidally dependent (~25 and 20 m during high and low tide), with lowest visibility occurring on the outgoing tide when lagoon waters flowed out of the channel (Fig. S5 in Supplement 3). During the daytime, at all camera locations, the *L. fulvus* aggregation movements were very dynamic and seemingly random, moving back and forth from shallow to deep and east to west. The orientation of the cameras (1 and 2 oriented up-wall, 3 and 4 oriented down-wall) could also potentially influence the detection of fish.

Overall, the number of *L. fulvus* increased as the full moon approached, was greatest the day after the full moon, and then decreased until the cameras were recovered (Fig. 4). Differences were seen in the presence of fish at different cameras, and are described for the 4 cameras (1 to 4) from east to west. For Camera 1, located furthest east and facing west, aggregating fish were present for a short period of time starting the day of the full moon in 2011 (Fig. 4a). Otherwise they were near-continuously present until 2 or 3 d after the full moon during daylight hours in both years (Fig. 4). Fish aggregations were almost always present at Camera 1 at dawn and almost always absent at dusk. Aggregations at this location were often shallower than the depth of the camera and occasionally out of view.

Camera 2 faced east, and aggregations were visible for a short time on the day before the full moon, and present near-continuously during daylight hours from the morning of the full moon until ~4 d after. Aggregations were the largest and most consistent at this location. Aggregations were often, but not always, absent during the last images at sunset of each day.

Camera 3 faced east, and aggregations were only present on 2 evenings in 2011 and most often after dawn and before dusk in 2012. A single fish, potentially the same individual, was periodically present throughout the entire 10 d deployment in 2012.

In 2012, Camera 4 (not present in 2011) was located furthest west, faced west, and had an unexpected battery failure midway through the study period. There were aggregations of fish photographed on the day of the full moon and the entire day after the full moon.

The time-lapse photos provided information on fish diel movements via presence–absence and body directional orientation. Overall, there were fewer fishes of all species present at dawn and dusk, but the status of the *L. fulvus* aggregation was often difficult to determine, as camera images were often too dark to discern occurrence. However, there were consistent patterns seen between cameras (Fig. 4). On most evenings, the images before dusk indicated the fish were absent before photos became too dark

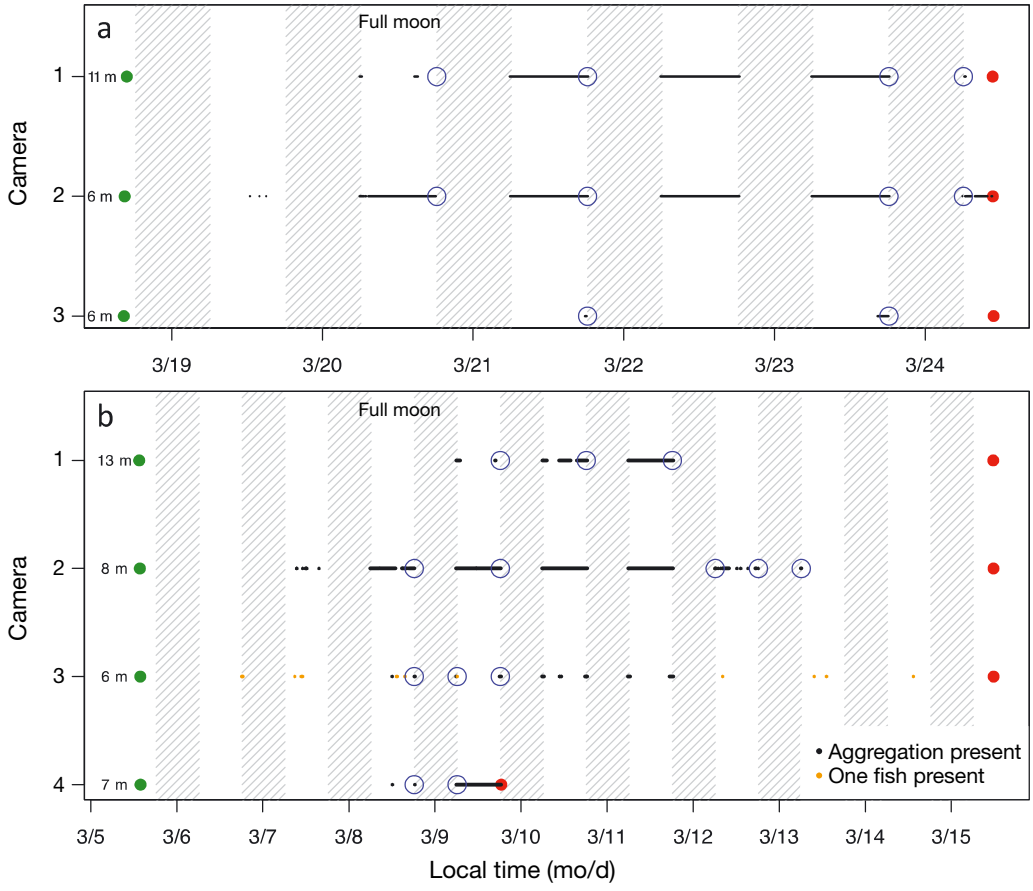


Fig. 4. Presence and absence of *Lutjanus fulvus* in time-lapse photos during March (a) 2011 and (b) 2012. Black points: the presence of a snapper aggregation; orange points: the presence of 1 fish. The beginning and end of the time-lapse photos on each camera are shown by the green and red points. Camera 4 unexpectedly turned off on 9 March 2012. Blue circles indicate the absence of an aggregation in the first or last photo of each day when an aggregation was recently present. The depth of each camera and date of the full moon is shown. Gray bars represent the period between sunset and sunrise

at sunset, and frequently, the swimming schools were oriented to the west a few meters deeper than the camera, noticeably deeper than their daytime distributions. On some mornings, the images at dawn indicated that groups of *L. fulvus* were absent. In general, fish numbers in the aggregation increased throughout the morning with the fish appearing to be arriving from the west. This movement pattern was especially apparent at Camera 3, where fish appeared to be only transiting through this area moving westward at sunset and eastward at sunrise.

### Aggregation distribution and channel flow characteristics

The REMUS was used on 4 d during the aggregation period on the outgoing tide to measure fish density and water properties. Physical measurements of water properties showed changes at different stages of the outgoing tide, but with overall low variability in temperature, salinity, and density (see Fig. S5 in Supplement 3 for comparison between REMUS mission time and tide). In general, the missions that started sooner after high tide (with current outgoing) had waters that were cooler (28.4°C), saltier (33.7 ppt) and denser (1021.3 kg $m^{-3}$), an indication of oceanic water characteristics brought in on the previous rising tide (Fig. S5 in Supplement 3). During missions that started later as the tide went out, waters were more lagoon-like, being slightly warmer (28.6°C), less salty (33.6 ppt), and less dense (1021.2 kg $m^{-3}$). To investigate the seasonal increase in temperature during summer months, a thermograph was deployed at the aggregation site at 15 m from January to May 2012. This showed similar measurements of 28 to 29°C from January to April, increasing to 29.5°C in May. During the summer in July 2010 (which was a

warmer than normal summer when coral bleaching occurred), the temperature range was 29.5 to 30.5°C.

We investigated the vertical, temporal, and spatial distribution of fish using the REMUS echosounder. The average target strength of single targets was –48.18 ± 5.68 dB at 217 kHz. It should be noted that a small calibration offset may be present, likely <2 dB (see Section S1 in Supplement 1). For the 4 profile depths (5, 9, 12/13, 18 m), the mean and standard deviation in fish density averaged over all survey days was the highest for mid-depths (9 and 13 m; Fig. 5) where fish density was significantly different ($p < 0.05$, multiple comparison test after Kruskal-Wallis test) between all depths except 9 and 13 m. The west and east ends of the survey had a low mean and standard deviation in fish density (1 ± 1 fish $m^{-2}$), indicating that since very few fish were present the limits of the aggregation had been reached. Fish density was higher and the aggregation spanned a wider horizontal range (up to 125 m distance) at intermediate depths (9 and 12/13 m, on average 2 ± 2 fish $m^{-2}$ and up to 11 ± 14 fish $m^{-2}$) compared to 5 and 18 m depths (Fig. 5). In general, the peak densities of fish on each day were between Cameras 2 and 3 (Fig. S6 in Supplement 3). The densities of fish were significantly different between all days (i.e. 9 and 21 March, 8 and 21 March, 8 and 9 March, 8 and 10 March, and 10 and 21 March) that were surveyed ($p < 0.05$, multiple comparison test after Kruskal-Wallis test) except for 9 and 10 March (Fig. S6). Spatially, the highest density of fish at each depth was found near the channel wall (Fig. S7 in Supplement 3) with the overall 'near wall' highest mean densities and standard deviations again between 9 and 12/13 m between Cameras 1 and 3 (Fig. S7).

When calculating the abundances of fish for each survey day in relation to the full moon, the minimum, average, and maximum abundances ranged from 635 to 3459, 3409 to 4576, and 5232 to 7911 individuals, respectively (Fig. S8 in Supplement 3). The minimum, average, and maximum values were calculated by kriging on a 5 m (horizontal) and 1 m (vertical) grid ranging from 3 to 20 m. Using these abundance estimates from all days, the average residence time of individuals (1.5 d), and total duration of the aggregation (6 d), we estimated that an average of 15 146 (min. 7046, max. 26 588) fish aggregated in West Channel during each full moon period during our surveys.

Fish densities were compared with current velocity at different distances from the channel wall (Fig. 6) to understand these relationships at this site. At high tide, current velocities were nearly 0 while at low tide, current velocities ranged from 0 at the channel wall to ~0.5 m $s^{-1}$ at 140 m from the channel wall (Fig. 6a). Therefore, at low tide, water still flowed out of West Channel because it is the only open conduit for transporting water between this region of the lagoon and barrier reef (the reef top is dry hence cannot transport water). On the incoming and outgoing tide, average current velocities from the channel wall to 140 m out from the wall ranged from ~0.05 to 1.1 and ~0.05 to 0.8 m $s^{-1}$, respectively. Fish were generally <30 m from the channel wall, with the majority of fish found between 0 and 15 m distance from the wall (Fig. 6b). At 15 m from the channel wall, currents were on average <0.25 m $s^{-1}$ while at 30 m from the

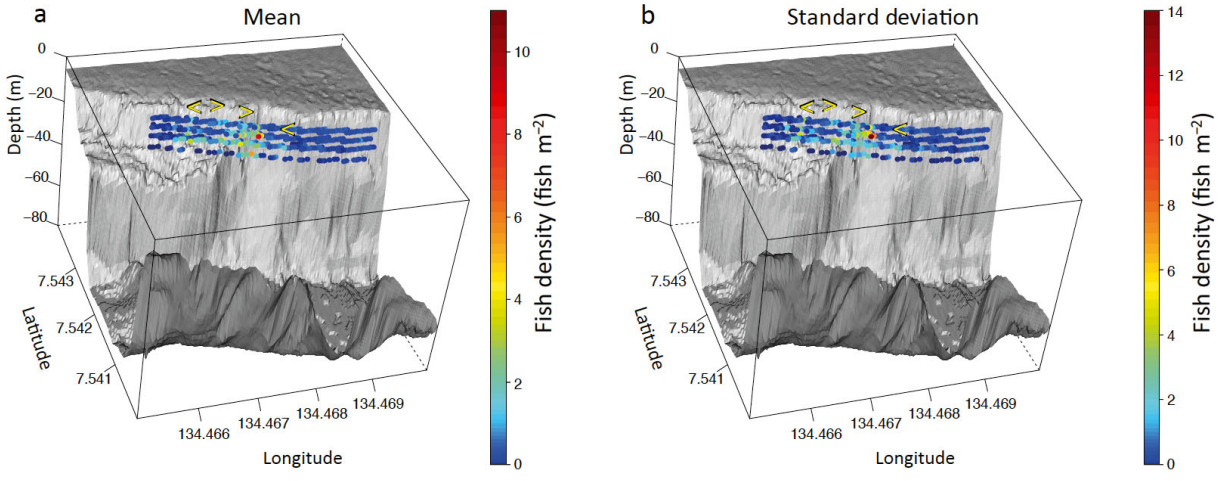


Fig. 5. *Lutjanus fulvus* density at various depths along the channel wall relative to 3D bathymetry. The (a) mean and (b) standard deviation in fish $m^{-2}$ for all REMUS missions at each depth. In 2012, transects were run at 5, 9,and 13 m depth. In 2011, transects were run at 5, 12, and 18 m. Transects at 12 and 13 m were grouped together. Yellow arrows represent locations of time-lapse cameras

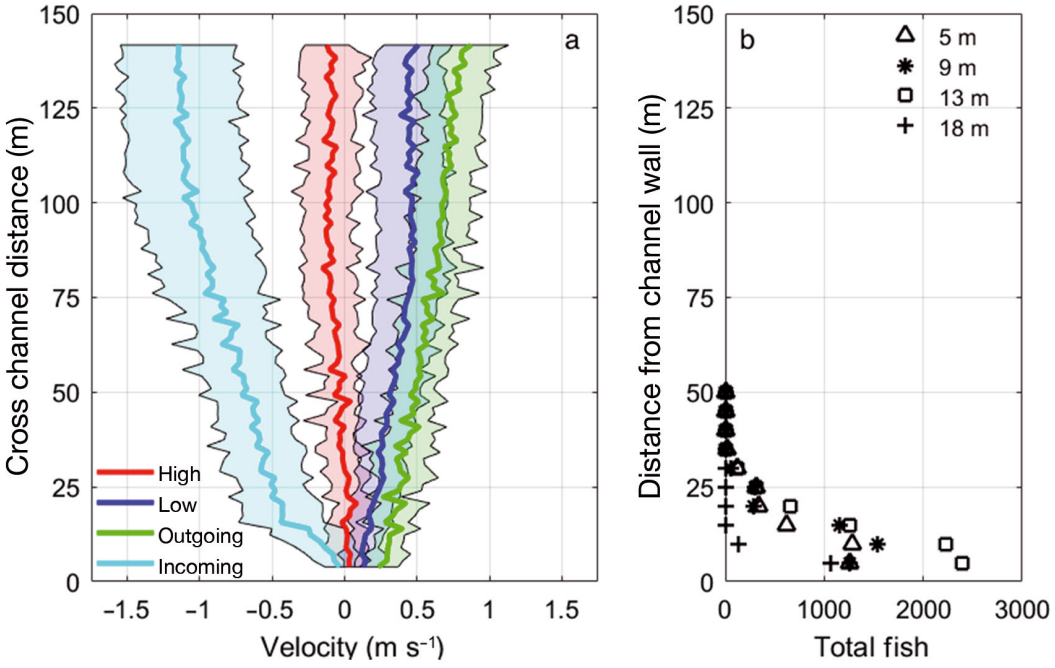


Fig. 6. Current velocity during different tidal phases, and total number of *Lutjanus fulvus* detected as a function of distance from the channel wall from all REMUS surveys. (a) Mean and standard deviation in current velocities during high, low, outgoing, and incoming tide from 0 to 150 m from the horizontal acoustic Doppler current profiler (HADCP) location on the channel wall. See Fig. S3 in Supplement 3 for tide phase identification. (b) Sum of the maximum number of fish detected at different distances from the channel wall for all REMUS surveys at 5 m (n = 4), 9 m (n = 3), 12/13 m (n = 4), and 18 m (n = 1); the number of sampling days at each depth is in parenthesis. All REMUS surveys occurred on the outgoing tide. Maximum fish density (fish $m^{-3}$) within 5 $m^2$ grid cells was determined for each survey on each sampling day (see Fig. S8 in Supplement 3). The densities of fish were grouped into distance bins from the channel wall to 50 m away from the wall in 5 m increments. The total number of fish across all surveys was then summed as a function of distance from the channel wall

wall, they were on average <0.6 m $s^{-1}$ on the incoming and <0.4 m $s^{-1}$ on the outgoing tide.

Because the HADCP was not located within the aggregation site, we compared its current velocities with those measured by the REMUS ADCP during the same tide phase (outgoing tide) and distance from the wall (~40 m; see Fig. S9 in Supplement 3). The mean current velocity during all REMUS missions was 0.53 m $s^{-1}$ while that for the HADCP was 0.52 m $s^{-1}$ (Fig. S9), providing confidence the REMUS and HADCP currents are comparable. There are, however, bathymetric differences between the aggregation site and the HADCP location that may locally influence flow. The HADCP was located to the west of a small indent (roughly 50 m) in the channel wall while the aggregation site is located east of an abrupt change in bathymetry where a shallow plateau (~40 m depth; Fig. 5) interrupts current flow along the channel wall (Figs. S9 & 1b).

Surface flow along the channel wall is likely affected by changes in bathymetry within West Channel. The time-lapse camera placed on an above-water pole on the south side of the channel (Fig. 1b) provided evidence of an eddy-like oceanographic feature that persisted from the time of deployment at 10:20 h until it dissipated as low tide approached at 14:55 h (see Fig. S10a,b in Supplement 3). At this location, there is an abrupt change in bathymetry along the channel wall that likely creates this feature, but only on the outgoing tide, which agrees with visual observations made at the aggregation site on the outgoing tide. We further mapped the flow near the aggregation site using drogues and uranine dye, which showed the surface waters flowed towards the middle of the channel and outwards towards the channel mouth (see Figs. S10 & S11, Table S3 in Supplement 3 and Section S4 in Supplement 1).

## DISCUSSION

Understanding species–habitat interactions is fundamental to understanding life-history strategies and protecting important habitat. Using a variety of instruments, we provide a description of *Lutjanus fulvus* movements within and across aggregation peri-

ods, in relation to the physical habitat and oceanography of West Channel. This aggregation was first discovered in 2007, has continued to form to the present (2017) and likely has a year-around presence (Sadovy de Mitcheson & Colin 2012, P. Colin unpubl. data). Around the time of the full moon each month, *L. fulvus* form a pre-spawning aggregation on the northern reef wall of a tidal channel, with extremely high site fidelity (within 10s of m). The aggregation has the highest densities from 9 to 13 m, spans 125 m within an indent in the channel wall, and is <15 m from the wall where current velocities are low. While spawning was never directly observed, movement patterns suggested *L. fulvus* migrate to a projection outside of the channel mouth to spawn after sunset on the outgoing tide and later return to the aggregation site. Understanding a species' movements and habitat utilization aids in creating adequate protected areas, which should include their aggregation site, migration corridors, and spawning area.

### Fish presence and potential reproduction timing

The timing (seasonal, lunar, diel) of spawning by fishes is an important component of reproductive success and may aid in entraining slightly buoyant eggs and larvae into water masses that increase their chance of survival in the pelagic realm (Donahue et al. 2015). We examined the presence of individual fish and aggregations across many temporal scales (months, days, hours) in relation to their surrounding habitat. It was known that *L. fulvus* aggregated within West Channel each month to spawn (Sadovy de Mitcheson & Colin 2012, P. Colin unpubl. data), but our study showed some individuals visited this aggregation site each full moon for at least 6 consecutive months. Based on the evidence of a year-round aggregation, it is likely some individual fish migrate to the aggregation site every month of the year. In Palau, there is no distinct seasonal cycle in productivity; rather, it is continuous and of low amplitude. Therefore, it is unlikely that there would be a feeding advantage to restricting spawning to the time of a seasonal bloom (match–mismatch hypothesis; Cushing 1990). Day length is also relatively consistent in Palau (~12 h), changing by less than 1 h between the winter and summer solstice (Colin 2012). Thus, the limited variability in annual water temperature and light in Palau makes for suitable spawning conditions year-round. Spawning each month could be an optimal strategy to maximize larval survival and enhance recruitment success (Lambert & Ware 1984).

*L. fulvus* aggregated each month during the time of the full moon from 1 d before to 4 d after, a total of 6 d (Figs. 3 & 4). During the full moon, tidal amplitudes and currents are greatest, and the full moon provides significant nocturnal light to a shallow reef environment, allowing fish to see quite well. In tidal channels of the Indo-west Pacific, many fish spawn after high tide when currents are moving towards the open ocean (Bell & Colin 1986, Colin 2012).

During full moon aggregation periods, time-lapse photos and acoustic telemetry data provided useful indications of *L. fulvus* diel movements. Our data suggest fish leave the aggregation site around sunset, migrate to the channel mouth, presumably spawn, and return by sunrise. Time-lapse photos revealed that fewer fish were present at dawn and dusk, and frequently showed groups swimming westward at dusk towards the channel mouth and eastward at dawn towards the aggregation site. Tagged fish were frequently detected during daytime at the aggregation site but detections decreased at night. Three fish were detected multiple times near the channel mouth after sunset near high tide. These fish were all detected at the channel mouth within the same time period, suggesting many other individuals were likely present. Other snappers with known spawning behavior (Sakaue et al. 2016) that do not aggregate in channels make daily migrations from 'resting areas' to spawn at promontories. Thus, if *L. fulvus* does migrate from inside the channel to spawn at its mouth, it differs from other snappers that are not associated with channels, but may be similar in having a migration from aggregation to spawning site. It is unclear what the fish are doing for the remainder of the night after migrating to the channel mouth, as we only have a few detections during this time. Snappers are typically nocturnally active fishes; therefore, it is possible they disperse after an early evening spawning to feed.

Spawning at night might be beneficial by limiting the effectiveness of visual predators. For some day-spawning species, piscivore and egg predators converge on the spawning sites to take advantage of these temporary but predictable sources of food (Nemeth 2012). Over our study period, early evening also coincides with highest outgoing flows from West Channel, helping to rapidly disperse eggs away from potential predators.

### Aggregation distribution and abundance

Active and passive acoustics and time-lapse photos were a means of assessing the temporal, vertical, and

spatial distribution of fish. They are a complementary and effective way to study a species that is very shy and not easy for divers/snorkelers to visually survey via standard methods. Acoustic data collected by the REMUS, surveying ~400 m of the channel wall, indicated the aggregation length was only about 125 m. Vertically, fish densities were highest at 9 to 13 m (compared to 5 and 18 m depth), and fish were close to the channel wall at all depths. Few fish were present beyond 25 m from the reef wall. Since the channel wall is sloping, at shallower depths, fish that were ~20 m from the channel wall may still be fairly close to the sloping bottom.

The area between Cameras 2 and 3, near receiver D, had the most consistent population of fish present during the full moon period (Fig. 4). This area also had the highest proportion of acoustic detections and peak densities in fish (see Fig. S6 in Supplement 3). These patterns of occurrence were highly consistent, given that the telemetry data was from November 2012 to March 2013, the time-lapse cameras were deployed for 1 or 2 wk, and REMUS missions spanned hours in March 2011 and 2012 (see Table S1 in Supplement 2). This extremely high site fidelity (10s of m) between years suggests conditions are ecologically stable and favorable over time, and perhaps provide daytime refuge similar to resting areas used by *Lutjanus bohar* and *Symphorichthys spilurus* (Sakaue et al. 2016) and courtship arenas documented for other snappers where males and females begin to interact before spawning occurs (Heyman et al. 2005, Kadison et al. 2006, Nemeth 2012).

Although this aggregation of *L. fulvus* has been known since 2007, no quantitative surveys of fish numbers have been made. At best, qualitative estimates of 10 000 to 20 000 fish in the aggregation were reported (Sadovy de Mitcheson & Colin 2012) based on rough values of fish density within the aggregation extrapolated over the estimated aggregation area. Fish abundance from the present acoustic surveys varied by day, and by summing the interpolated mean abundance across the survey area, it was estimated that 3500 to 4000 fish were present on the day of the full moon and 1 d after, and slightly higher 2 d after (4500). Given the high mobility of the aggregation, as seen in time-lapse photos, moving frequently from shallow to deep and east to west, it is possible the acoustic surveys underestimated the total number of fish present at the site. When the REMUS ran consecutive survey lines alternating between depths, it was not uncommon to have transects at the same depth with variable density estimates, ranging from no fish to 14 fish $m^{-2}$ at the same location. Therefore, it is possible the aggregation abundance is between our estimates (approx. 4000 fish $d^{-1}$) and visual surveys (20 000) (Sadovy de Mitcheson & Colin 2012). It is also possible that the total number of fish that visit the aggregation site varies month-to-month, as we found all tagged fish did not return each month. Accounting for the residence time of individual fish (1.5 d) and total duration of the aggregation (6 d), we estimated ~15 000 fish aggregated in West Channel each full moon during our study. In comparison, the typical abundance of *L. fulvus* outside of the spawning period is normally only a handful of fish (Sadovy de Mitcheson & Colin 2012). Such high peaks in fish density (i.e. 'hot moments') can have cascading effects on food web dynamics, nutrient cycling, and energy transfer through feeding and defecation by spawners, and predation on spawners and their eggs (Archer et al. 2015).

A limited number of bioacoustic studies have measured the abundance of spawning aggregations from surface vessels. In these studies, the results have been variable, with some producing radical overestimates (Ehrhardt & Deleveaux 2007), while others did not discriminate between species (Johnston et al. 2006). Egerton et al. (2017) produced one of the first reasonable acoustic studies of population size of a Nassau grouper *Epinephelus striatus* spawning aggregation, including visual surveys for validation. Our study is the first to use an AUV for such measurements, and we confirmed the composition of the fish community with visual observations and photographs. An AUV is likely less disruptive than a boat-based survey because it is relatively quiet, small, and transits quickly through the aggregation area. The AUV was also useful because the aggregation site was in a very difficult area to survey, occurring within a small area reaching into shallow water and on a steep reef slope, which could prove difficult and hazardous for boat surveys.

### Importance of the physical habitat to fish in West Channel

The extreme rarity of spawning aggregations and their high site fidelity suggests fish are attracted to specific features that are limited in availability (Colin 2012). For instance, hydrographic conditions may promote the transport of spawned eggs into new habitats, or allow for larval retention in suitable areas (Johannes 1978, Hamner & Largier 2012). We studied flow within West Channel by measuring current velocities, and releasing surface drifters and uranine dye. We found current velocities ranged from near 0 to 1.5 m $s^{-1}$ from

the wall to the middle of the channel, respectively (Fig. 6). However, the interaction between bathymetry and current flow may alter flow speeds, which suggests currents measured on the HADCP may not be fully representative of conditions at the aggregation site. Visual observations revealed an eddy-like feature at aggregation site (similar to Fig. S10a,b in Supplement 3). Our attempt to study flow within this feature using drifters and dye provided limited information besides flow within the eddy-like feature could be counterclockwise (Fig. S12 in Supplement 3). Dye released upstream from the feature in Expt 1 (Fig. S11a in Supplement 3) did not enter the eddy and dye released within the feature in Expt 2 (Fig. S11b) was immediately swept towards middle of channel. These results and visual observations suggest the feature is likely an upwelling that results from flow on the outgoing tide hitting a shallow, abrupt change in bathymetry. Fish are perceptive of their environment, and we speculate that this topographic change or current anomaly may be something the fish can sense (Derby & Sorensen 2008). We hypothesize that this feature could provide shelter (similar to Sakaue et al. 2016), or that it may not have any physical or biological benefits but rather acts as a signal to aggregate at this location.

To arrive at an aggregation site, fish often use predictable migration routes, such as shelf edges, drop-offs or channels. For example, some resident and transient aggregating species have known migration pathways between spawning and home/feeding sites (Colin 1996, Mazeroll & Montgomery 1998, Whaylen et al. 2004, Hutchinson & Rhodes 2010). Interestingly, there were very few detections on outer aggregation site receivers A and E, indicating fish were not traveling at shallow depths along the wall. Fish 5 and 7 were each detected for the last time in a spawning period at receiver G (Table 2), suggesting some fish may exit through the channel mouth. Telemetered fish arrived at the aggregation site between 02:00 and 06:00 h, and were last detected at the aggregation site between 14:00 and 18:00 h (Table 1), both during incoming tides. We hypothesize that fish are not swimming with the tide, but rather are swimming at deeper depths along the channel wall following the 30 m depth contour or deeper. In this case, fish arriving at the aggregation site would be out of the detection range of receiver A due to the change in slope of the channel wall, whereas the 30 m contour is well within range of receivers B and E (Fig. 1b). Regardless of the entrance or exit corridor, the fish move precisely, arriving and departing within the detection range of receivers B to D and Camera 2 without being detected on receivers A or E.

Many reef fish spawn at the mouth and inner reaches of reef channels, on top of or on the outer slope of a reef shelf edge (Nemeth 2009). Those with aggregations may occur along reef sections with or without prominent seaward projections or promontories (Colin 2012). We hypothesize *L. fulvus* moved to the channel mouth to spawn where there is a seaward projection on the north side of the channel beyond receivers G and H (Fig. 1). The southern side of the channel mouth lacks a similar structure, which may explain why the aggregation forms only on the north side.

### Understanding FSAs and implications for effective management

Our study has expanded our understanding of snapper spawning aggregation characteristics across many spatio-temporal scales, and in general, our hypotheses and findings are in agreement with past observations. Previously, snappers have been considered a transient aggregating species that are widely dispersed, solitary individuals, with spawning sites that could be many 10s of km away from their home ranges in the non-reproductive period, and with 2 or more short spawning periods per year (Nemeth 2012). New studies in the western Pacific suggest that most spawning adults do not travel far during non-reproductive periods, given the high temporal frequency (monthly) of aggregations and their common occurrence on most reefs. Given the timing and frequency of the *L. fulvus* aggregation (lunar phased, but with year-round spawning), they appear to have elements of both transient and resident, similar to *L. bohar* (Sakaue et al. 2016).

Considering that *L. fulvus* are not present at their spawning or aggregation site for about 85% of each lunar month, future studies should investigate their home range outside of the spawning period, and work to quantify their distribution and abundance at the proposed spawning site. This information is vital for protecting a fish throughout its entire range. Marine Protected Areas should ideally include the entire catchment area (migration routes, courtship arena, and spawning grounds) to most effectively manage a species (Sadovy de Mitcheson & Erisman 2012). The health of a FSA is an indicator of population health (Gascoigne 2002), where any decrease in abundance would have negative consequence for reproductive output. Overall, studying the dynamics of FSA sites across many spatio-temporal scales provides necessary information for understanding the health and ensuring the long-term sustainability of a species.

*Acknowledgements.* This research was supported by the National Geographic Society/Waitt Grants Program (2281-2) and the US Office of Naval Research Flow Encountering Abrupt Topography, Department Research Initiative. M.C. was partially supported through the generous funding of the Friedkin Foundation. We thank the Palau Community College aquaculture program for use of their hatchery facility for holding fish and acknowledge Jon Vogt for his assistance and logistical support. Emilio Basilius, Lori Colin, Amy Grace, Matt Mesubed, William Middleton, Sharon Patris, Shannon Scott, and Gerda Ucharm assisted with the field work and tagging.

## LITERATURE CITED

Aglen A (1989) Empirical results on precision-effort relationships for acoustic surveys. ICES CM 1989/B30. ICES, Copenhagen

Allen GR, Talbot FH (1985) Review of the snappers of the genus *Lutjanus* (Pisces: Lutjanidae) from the Indo-Pacific, with the description of a new species. Indo-Pac Fish 11:1–87

Archer SK, Allgeier JE, Semmens BX, Heppell SA and others (2015) Hot moments in spawning aggregations: implications for ecosystem-scale nutrient cycling. Coral Reefs 34:19–23

Bacheler NM, Whitfield PE, Muñoz RC, Harrison BB, Harms CA, Buckel CA (2015) Movement of invasive adult lionfish *Pterois volitans* using telemetry: importance of controls to estimate and explain variable detection probabilities. Mar Ecol Prog Ser 527:205–220

Bell LJ, Colin PL (1986) Mass spawning of *Caesio teres* (Pisces: Caesionidae) at Enewetak Atoll, Marshall Islands. Environ Biol Fishes 15:69–74

Bezerra-Neto JF, Brighenti LS, Pinto-Coelho RM (2013) Implementation of hydroacoustic for a rapid assessment of fish spatial distribution at a Brazilian Lake-Lagoa Santa, MG. Acta Limnol Bras 25:91–98

Breece MW, Oliver MJ, Cimino MA, Fox DA (2013) Shifting distributions of adult Atlantic sturgeon amidst post-industrialization and future impacts in the Delaware River: a maximum entropy approach. PLOS ONE 8: e81321

Colin PL (1996) Longevity of some coral reef fish spawning aggregations. Copeia 1996:189–192

Colin PL (2009) Marine environments of Palau. Indo-Pacific Press, San Diego, CA

Colin PL (2012) Timing and location of aggregation and spawning in reef fishes. In: Sadovy de Mitcheson Y, Colin PL (eds) Reef fish spawning aggregations: biology, research and management. Springer, New York, NY, p 117–158

Cressie N (1988) Spatial prediction and ordinary kriging. Math Geol 20:405–421

Cushing DH (1990) Plankton production and year-class strength in fish populations: an update of the match/mismatch hypothesis. Adv Mar Biol 26:249–293

Dalen J, Nakken O (1983) On the application of the echo-integration method. ICES CM 1983/B:19. ICES, Copenhagen

Derby CD, Sorensen PW (2008) Neural processing, perception, and behavioral responses to natural chemical stimuli by fish and crustaceans. J Chem Ecol 34:898–914

Domeier ML (2012) Revisiting spawning aggregations: definitions and challenges. In: Sadovy de Mitcheson Y, Colin P (eds) Reef fish spawning aggregations: biology, research and management. Springer, New York, NY, p 1–20

Domeier ML, Colin PL (1997) Tropical reef fish spawning aggregations: defined and reviewed. Bull Mar Sci 60: 698–726

Donahue MJ, Karnauskas M, Toews C, Paris CB (2015) Location isn't everything: timing of spawning aggregations optimizes larval replenishment. PLOS ONE 10: e0130694

Egerton JP, Johnson AF, Le Vay L, McCoy CM, Semmens BX, Heppell SA, Turner JR (2017) Hydroacoustics for the discovery and quantification of Nassau grouper (*Epinephelus striatus*) spawning aggregations. Coral Reefs 36:589–600

Ehrhardt NM, Deleveaux VKW (2007) The Bahamas' Nassau grouper (*Epinephelus striatus*) fishery—two assessment methods applied to a data-deficient coastal population. Fish Res 87:17–27

Gascoigne J (2002) Nassau grouper and queen conch in the Bahamas: status and management options. Bahamas Reef Environment Educational Foundation. Nassau, The Bahamas

Hamner WM, Largier JL (2012) Oceanography of the planktonic stages of aggregation spawning reef fishes. In: Sadovy de Mitcheson Y, Colin PL (eds) Reef fish spawning aggregations: biology, research and management. Springer, New York, NY, p 159–190

Heyman WD, Kjerfve B (2008) Characterization of transient multi-species reef fish spawning aggregations at Gladden Spit, Belize. Bull Mar Sci 83:531–551

Heyman WD, Kjerfve B, Graham RT, Rhodes KL, Garbutt L (2005) Spawning aggregations of *Lutjanus cyanopterus* (Cuvier) on the Belize barrier reef over a 6 year period. J Fish Biol 67:83–101

How JR, de Lestang S (2012) Acoustic tracking: issues affecting design, analysis and interpretation of data from movement studies. Mar Freshw Res 63:312–324

Hutchinson N, Rhodes KL (2010) Home range estimates for squaretail coralgrouper, *Plectropomus areolatus* (Rüppell 1830). Coral Reefs 29:511–519

Johannes RE (1978) Reproductive strategies of coastal marine fishes in the tropics. Environ Biol Fishes 3:65–84

Johannes RE (1981) Words of the lagoon: fishing and marine lore in the Palau district of Micronesia. University of California Press, Berkeley, CA

Johnston SV, Rivera JA, Rosario A, Timko MA, Nealson PA, Kumagai KK (2006) Hydroacoustic evaluation of spawning red hind (*Epinephelus guttatus*) aggregations along the coast of Puerto Rico in 2002 and 2003. In: Taylor JC (ed) Emerging technologies for reef fisheries research and management. NOAA Prof Pap NMFS 5. Scientific Publications Office, Washington, DC, p 10–17

Journel AG, Huijbregts CJ (1978) Mining geostatistics. Academic Press, New York, NY

Kadison E, Nemeth RS, Herzlieb S, Blondeau J (2006) Temporal and spatial dynamics of *Lutjanus cyanopterus* (Pisces: Lutjanidae) and *L. jocu* spawning aggregations in the United States Virgin Islands. Rev Biol Trop 54: 69–78

Kawabata Y, Asami K, Kobayashi M, Sato T and others (2011) Effect of shelter acclimation on the post-release movement and putative predation mortality of hatchery-reared black-spot tuskfish *Choerodon schoenleinii*, de-

termined by acoustic telemetry. Fish Sci 77:345
Lambert TC, Ware DM (1984) Reproductive strategies of demersal and pelagic spawning fish. Can J Fish Aquat Sci 41:1565–1569
Mazeroll AI, Montgomery WL (1998) Daily migrations of a coral reef fish in the Red Sea (Gulf of Aqaba, Israel): initiation and orientation. Copeia 1998:893–905
Moline MA, Blackwell SM, Von Alt C, Allen B and others (2005) Remote environmental monitoring units: an autonomous vehicle for characterizing coastal environments. J Atmos Ocean Technol 22:1797–1808
Nemeth RS (2005) Population characteristics of a recovering US Virgin Islands red hind spawning aggregation following protection. Mar Ecol Prog Ser 286:81–97
Nemeth RS (2009) Dynamics of reef fish and decapod crustacean spawning aggregations: underlying mechanisms, habitat linkages, and trophic interactions. In: Nagelkerken I (ed) Ecological connectivity among tropical coastal ecosystems. Springer, New York, NY, p 73–134
Nemeth RS (2012) Ecosystem aspects of species that aggregate to spawn. In: Sadovy de Mitcheson Y, Colin PL (eds) Reef fish spawning aggregations: biology, research and management. Springer, New York, NY, p 21–55
Özgül A, Lök A, Ula A, Düzbastılar FO, Tanrıkul TT, Pelister C (2015) Preliminary study on the use of the VEMCO positioning system to determine fish movements in artificial reef areas: a case study on *Sciaena umbra linnaeus*. J Appl Ichthyology 31:41–47
Pinheiro J, Bates D, Debroy S, Sarkar D (2010) nlme: linear and nonlinear mixed effect models. R package version 31-102
R Core Team (2013) R: a language and environment for statistical computing. R Foundation for Statistical Computing, Vienna
Ribeiro PJJ, Diggle PJ (2001) geor: a package for geostatistical analysis. R News 1:15–18
Rogowski P, Terrill E, Chen J (2014) Observations of the frontal region of a buoyant river plume using an autonomous underwater vehicle. J Geophys Res C Oceans 119:7549–7567
Sadovy Y (2007) Report on current status and exploitation history of reef fish spawning aggregations in Palau. Western Pacific fishery survey series: Society for the Conservation of Reef Fish Aggregations, Vol 3. Palau Conservation Society, Koror
Sadovy Y, Domeier M (2005) Are aggregation-fisheries sustainable? Reef fish fisheries as a case study. Coral Reefs 24:254–262
Sadovy de Mitcheson Y, Colin PL (2012) Appendix: species that form spawning aggregation. In: Sadovy de Mitcheson Y, Colin PL (eds) Reef fish spawning aggregations: biology, research and management. Springer, New York, NY, p 595–604
Sadovy de Mitcheson Y, Erisman B (2012) Fishery and biological implications of fishing spawning aggregations and the social and economic importance of aggregating fishes. In: Sadovy de Mitcheson Y, Colin PL (eds) Reef fish spawning aggregations: biology, research and management. Springer, New York, NY, p 225–284
Sakaue J, Akino H, Ida H (2012) The blue-lined sea bream—*Symphorichthys spilurus*. In: Sadovy de Mitcheson Y, Colin PL (eds) Reef fish spawning aggregations: biology, research and management. Springer, New York, NY, p 468–472
Sakaue J, Akino H, Endo M, Ida H, Asahida T (2016) Temporal and spatial site sharing during spawning in snappers *Symphorichthys spilurus* and *Lutjanus bohar* (Pisces: Perciformes: Lutjanidae) in waters around Peleliu Island, Palau. Zool Stud 55:1–15
Sala E, Ballesteros E, Starr RM (2001) Rapid decline of Nassau grouper spawning aggregations in Belize: fishery management and conservation needs. Fisheries (Bethesda, Md) 26:23–30
Venables WN, Ripley BD (2002) Modern applied statistics with S, 4th edn. Springer, New York, NY
Whaylen L, Pattengill-Semmens CV, Semmens BX, Bush PG, Boardman MR (2004) Observations of a Nassau grouper (*Epinephelus striatus*) spawning aggregation site in Little Cayman Island. Environ Biol Fishes 70: 305–313

*Editorial responsibility: Myron Peck, Hamburg, Germany*

*Submitted: January 9, 2018; Accepted: May 31, 2018*
*Proofs received from author(s): August 2, 2018*